The Canadian Mineralogist
Vol. 35, pp. 313-326 (1997)

ORIGIN OF HIGH-An PLAGIOCLASE IN TONGAN HIGH-Ca BONINITES: IMPLICATIONS FOR PLAGIOCLASE–MELT EQUILIBRIA AT LOW P(H_2O)

LEONID V. DANYUSHEVSKY[1]

Department of Geology, University of Tasmania, GPO Box 252-79, Hobart, Tasmania, 7001, Australia

MICHAEL R. CARROLL

Department of Geology, University of Bristol, Bristol BS8 1RJ, U.K.

TREVOR J. FALLOON

Department of Geology, University of Tasmania, GPO Box 252-79, Hobart, Tasmania, 7001, Australia

ABSTRACT

Detailed petrological, mineralogical and melt-inclusion studies of an unusual plagioclase-phyric high-Ca boninite from the North Tongan forearc demonstrate that phenocrysts of high-An plagioclase ($An_{>90}$) crystallized at the latest stages of melt evolution from H_2O-saturated dacitic melts (64–67 wt.% SiO_2, ~2 wt.% MgO) at ~1050°C and low pressure (< 1 kbar). These melts contained ~1.5 wt.% H_2O and had low CaO/Na_2O (~3, in wt.%). Our results suggest that the presence of high-Ca ($An_{>90}$) plagioclase phenocrysts in arc lavas does not necessarily imply either high H_2O-contents of the melt (>6 wt.%), or involvement of refractory melts ($CaO/Na_2O > 8$) in magma genesis, as was previously suggested. Established conditions of crystallization [P, T, *X*, *X*(H_2O)] during evolution of the Tongan boninite contradict those predicted by available models of plagioclase–melt equilibria. The effect of H_2O on the activities of plagioclase components in hydrous melts is strongly nonlinear. Extrapolation of experimental results on the effect of H_2O on plagioclase–melt equilibria from melt H_2O contents of >4 wt% to the low H_2O contents (<2 wt%) of the evolved Tongan boninite predicts a less calcic plagioclase than observed, or higher H_2O contents than measured in plagioclase-hosted melt inclusions. These observations are in accord with the well-known large effect of small amounts of H_2O on mineral melting temperatures, and also with recent results on the effect of H_2O on melt viscosities at low H_2O contents. Better predictions require new experimental data at low P(H_2O) (<1 kbar).

Keywords: high-An plagioclase, boninite, H_2O content, melt inclusions, plagioclase–melt equilibria, model, Tonga forearc.

SOMMAIRE

Une étude détaillée fondée sur la pétrologie, la minéralogie et la composition des inclusions vitreuses de phénocristaux de plagioclase très calcique d'une boninite anomale de l'avant-arc du secteur nord de Tonga démontre que le plagioclase s'est formé aux stades ultimes de cristallisation, à partir d'un magma dacitique saturé en H_2O (64–67% de SiO_2, ~2% de MgO, en poids) à environ 1050°C et à faible pression (<1 kbar). De tels magmas contenaient ~1.5% en H_2O et avaient un faible rapport CaO/Na_2O (~3, en termes pondéraux). D'après nos résultats, la présence de phénocristaux de plagioclase très calcique ($An_{>90}$) ne requiert pas nécessairement des teneurs en H_2O du magma très élevées (>6%, par poids) ou l'implication d'un magma réfractaire ($CaO/Na_2O > 8$), comme il est généralement supposé. Les conditions de cristallisation préconisées [P, T, *X*, *X*(H_2O)] au cours de l'évolution de la boninite de Tonga contredisent celles qui sont prédites à partir des modèles disponibles de l'équilibre entre plagioclase et magma. L'influence de H_2O sur l'acivité des composantes du plagioclase dans les magmas est fortement non linéaire. Une extrapolation des résultats expérimentaux sur l'effet de H_2O sur l'équilibre plagioclase–liquide, établi pour des teneurs de H_2O supérieures à 4% (poids), aux faibles teneurs (<2%) observées dans le cas de la boninite évoluée, predit un plagioclase moins fortement calcique que ce qui est observé, ou bien une teneur en H_2O plus élevée que celle qui est mesurée dans les inclusions vitreuses piégées par le plagioclase. Nos observations concordent bien avec l'influence très marquée de faibles quantités de H_2O sur le point de fusion des minéraux, et avec les résultats récents de l'effet de H_2O sur la viscosité des magmas à faibles teneurs en H_2O. De meilleures prédictions imposent de nouvelles données expérimentales obtenues à faible P(H_2O) (<1 kbar).

(Traduit par la Rédaction)

Mots-clés: plagioclase calcique, boninite, teneur en H_2O, reliquats magmatiques, équilibre plagioclase–liquide, modèle, avant-arc de Tonga.

---

[1] *E-mail address*: l.dan@geol.utas.edu.au

INTRODUCTION

The origin of calcic plagioclase ($An_{>90}$) in arc-related and mid-ocean ridge basalts has received considerable attention (Falloon & Green 1986, Housh & Luhr 1991, Fram & Longhi 1992, Sisson & Grove 1993, Sinton *et al.* 1993, Panjasawatwong *et al.* 1995, Kimata *et al.* 1995). Experimental studies of plagioclase–melt equilibria have demonstrated that melt Al/Si and Ca/Na values and H_2O contents are the most important parameters affecting the composition of plagioclase on the liquidus. An increase in any of these compositional parameters results in crystallization of more calcic plagioclase. For anhydrous tholeiitic systems, high-An plagioclase ($An_{>90}$) can crystallize from high-Al (>16–17 wt.% Al_2O_3, $Al_2O_3/SiO_2 > 0.32$, in wt.%) and high CaO/Na_2O (>8, in wt.%) melts. H_2O-rich andesitic and dacitic melts at pressures of 2–5 kilobars (>6 wt.% H_2O) can crystallize An-rich plagioclase at $CaO/Na_2O \approx 4–5$ and relatively low Al_2O_3/SiO_2 values (<0.25). The effects of H_2O-undersaturated conditions, and total H_2O pressures less than 2 kilobars on plagioclase–melt equilibria remain poorly constrained. There exist some experimental data (Baker & Eggler 1987, Panjasawatwong *et al.* 1995) to suggest that H_2O-undersaturated conditions have less effect on compositions of liquidus plagioclase than H_2O-saturated conditions (given similar amounts of H_2O in the melt), but there are very few data on plagioclase–melt equilibria at total H_2O pressures less than 2 kilobars.

Our new observations concerning high-An plagioclase phenocrysts in the North Tongan high-Ca boninitic suite (Falloon & Green 1986, Falloon & Crawford 1991) are of particular interest because current models of plagioclase–melt equilibria do not predict the crystallization of such An-rich plagioclase from these high-Ca boninitic melts. As can be inferred from the presence of H_2O-rich primary fluid inclusions in all phenocryst phases (olivine, pyroxenes and plagioclase), these magmas crystallized at conditions close to H_2O-saturation (Danyushevsky *et al.* 1995, Sobolev & Danyushevsky 1994), and differentiation was accompanied by continuous degassing. The H_2O content of primitive high-Mg melts from this suite, trapped as melt inclusions in olivine, is 2.5–3 wt.%, and decreases to ~1.5 wt.% in evolved dacitic melts, implying low-pressure (<1 kilobar) conditions over the entire recorded history of crystallization. Primitive melts from this suite have sufficiently high CaO/Na_2O values (>10) to allow crystallization of high-An plagioclase, but the low Al_2O_3 (8–10 wt.%) and significant H_2O (2–3 wt.%) in such melts result in a lack of saturation of plagioclase until much lower temperatures. The evolved, plagioclase-saturated melts of this suite have low CaO/Na_2O values (~3) owing to extensive prior crystallization of clinopyroxene, and relatively low H_2O contents (~1.5 wt.%) due to degassing during ascent and eruption on the seafloor.

In this paper, we present a mineralogical and experimental study of melt inclusions, and infer the conditions of crystallization of high-An plagioclase from Tongan boninitic melts. Our results on these unique samples raise significant questions concerning the applicability of current models of plagioclase–melt equilibrium to boninite petrogenesis, and in general to plagioclase crystallization at low $P(H_2O)$ conditions (<1 kbar).

ANALYTICAL AND EXPERIMENTAL TECHNIQUES

Compositions of minerals and glasses were analyzed using a Cameca SX50 electron microprobe at the University of Tasmania, Hobart, at 15 kV and 20 nA, using international standards USNM 111240/2 (basaltic glass), USNM 122142 (augite), USNM 111312/444 (olivine), and USNM 115900 (plagioclase) (Jarosewich *et al.* 1980). Counting times for all elements were 10 s, and the beam size was ~1 μm for minerals, ~5 μm for glass. A comparison of Na_2O values obtained from analyses with beam currents of 20 and 10 nA demonstrates Na loss of ~0.1 wt.% Na_2O due to sample instability under the beam, which is approximately the same for glass analyzed in this study and anhydrous basaltic glass; all analyses have been corrected for this effect. The small magnitude of this correction is in accord with the findings of Nielsen & Sigurdsson (1981) that Na mobility is less of a problem in hydrous basaltic glass than in hydrous rhyolitic glass. Host-mineral compositions reported here were analyzed at ~20 μm distance from glass inclusions, normally on several different sides of the inclusions.

H_2O concentrations in glass inclusions were analyzed by FTIR spectroscopy, using an IR microscope with all-reflecting optics; the calibration and procedures of Danyushevsky *et al.* (1993) were followed, including use of a standard (A-46) with a major-element composition similar to that of glasses analyzed in this study. Doubly-polished sections of phenocrysts (30–50 μm thick) were prepared with areas of glass inclusions >40 μm in diameter opened to the surface on each side. The diameter of the analyzed areas was restricted to 30 μm to ensure that no host plagioclase was present in the analyzed volume. Inclusions for FTIR analysis were selected using the following criteria: 1) entrapment during crystal growth (primary inclusions); this was determined by the position of the inclusion within the crystal, and by its negative crystal or oval shape [see Roedder (1984) for a detailed discussion]; 2) efficient quenching; only inclusions without a shrinkage bubble were selected (note that in hydrous systems, the shrinkage bubble is filled with fluid originally dissolved in the trapped melt); 3) "unopened" inclusions; the absence of a bubble in a hydrous melt inclusion is in itself a good indication that this inclusion has not experienced "leakage" after trapping, as the pressure drop associated with such an event would lead to vesiculation. In addition, inclusions

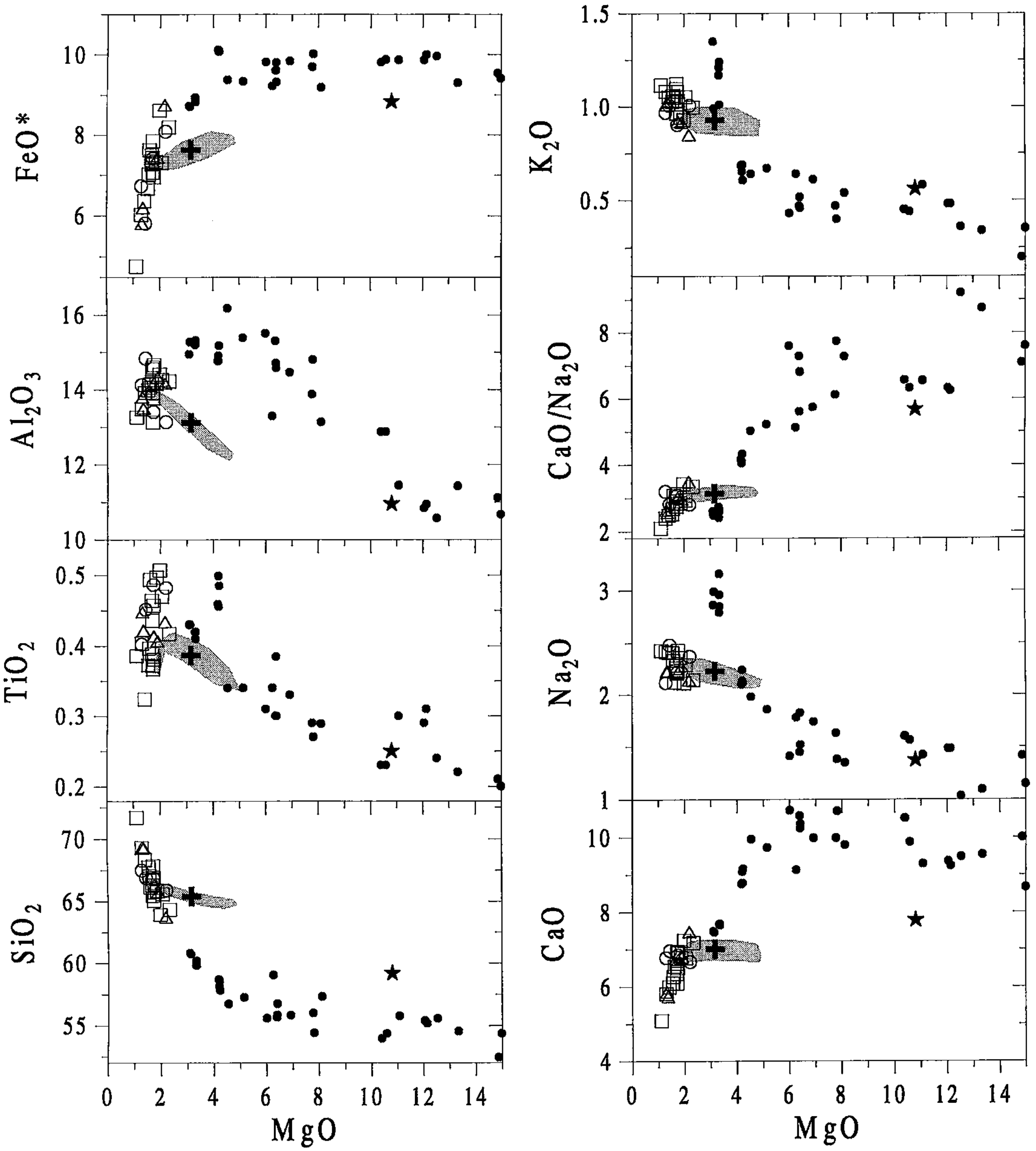

FIG. 1. Comparison of the compositions of melt inclusions in plagioclase phenocrysts from sample 3–24 with the compositions of rocks and matrix glass of the North Tongan suite of high-Ca boninite dredged from station 21, dredge haul 3. Dots: compositions of rocks and glasses from station 21 (Falloon & Crawford 1991). Star: sample 3–24. Open circles: matrix glass from sample 3–24. Squares: naturally quenched glass inclusions in plagioclase phenocrysts. Triangles: homogenized and quenched glass inclusions in plagioclase phenocrysts. Cross: groundmass composition of sample 3–24 estimated as an average result of 12 randomly positioned broad-beam (30 × 50 μm) electron-microprobe analyses; highlighted area around the groundmass composition represents variations of individual groundmass compositions caused by varying proportions between pyroxene microlites and the matrix glass.

TABLE 1. COMPOSITIONS OF GROUNDMASS, MATRIX GLASS, AND GLASS INCLUSIONS IN PLAGIOCLASE PHENOCRYSTS FROM SAMPLE 3-24*

	1	2	3	4	5	6	7	8	9	10	11	12	13	14	15	16	17	18	19
	GM	21	14	20	43	PL1	PL10	PL12	PL21	PL28	PL30	PL34	PL35	PL64	P-2	P-6	P-7	P-8	P-10
SiO_2	65.14	65.65	66.67	66.05	67.09	71.19	68.72	66.96	65.25	64.08	64.13	63.30	67.55	63.01	68.95	64.72	69.61	65.65	63.10
TiO_2	0.39	0.48	0.45	0.48	0.40	0.38	0.40	0.37	0.38	0.45	0.46	0.41	0.32	0.50	0.42	0.40	0.45	0.41	0.43
Al_2O_3	13.06	13.08	14.79	13.24	14.04	13.16	13.37	12.96	13.58	14.38	13.95	14.00	13.76	14.21	13.44	14.10	13.85	14.04	14.02
FeO	7.59	8.05	5.79	7.32	6.68	4.73	5.97	7.34	7.10	7.73	7.14	8.06	6.29	8.49	6.16	7.32	5.83	7.21	8.66
MnO	0.13	0.08	0.04	0.07	0.06	0.08	0.06	0.04	0.11	0.10	0.10	0.14	0.07	0.18	0.12	0.07	0.06	0.07	0.19
MgO	3.15	2.21	1.45	1.73	1.29	1.11	1.29	1.69	1.66	1.71	2.01	2.30	1.40	1.95	1.36	1.87	1.33	1.74	2.16
CaO	6.97	6.63	6.93	6.75	6.72	5.05	5.76	6.01	6.20	6.83	6.61	7.06	5.92	7.13	5.71	6.68	5.88	6.65	7.39
Na_2O	2.22	2.36	2.47	2.19	2.10	2.41	2.40	2.18	2.18	2.18	2.24	2.11	2.38	2.08	2.22	2.24	2.23	2.20	2.12
K_2O	0.92	1.00	1.00	0.89	0.96	1.11	1.07	1.11	1.07	0.95	1.03	0.98	1.04	0.92	1.02	0.90	1.01	0.91	0.84
P_2O_5	n.d.	0.11	0.11	0.11	0.08	0.08	0.11	0.06	0.13	0.09	0.10	0.04	0.10	0.11	0.12	0.07	0.09	0.11	0.11
H_2O	n.d.	n.d.	n.d.	n.d.	n.d.	n.d.	n.d.	n.d.	1.50	n.d.	1.40	1.60	n.d.	n.d.	n.d.	n.d.	n.d.	n.d.	n.d.
Total	99.59	99.65	99.70	98.83	99.42	99.31	99.20	98.71	99.16	98.50	99.17	100.0	98.83	98.58	99.52	98.37	100.34	98.99	99.02
Mg#	44.87	35.23	33.16	31.89	27.67	31.47	29.71	31.16	31.65	30.47	35.80	36.11	30.60	31.10	30.43	33.60	31.13	32.34	33.07
CaO/Na_2O	3.1	2.8	2.8	3.1	3.2	2.1	2.4	2.8	2.8	3.1	3.0	3.3	2.5	3.4	2.6	3.0	2.6	3.0	3.5
Host An						83.7	85.7	89.0	89.3	94.1	92.0	91.9	88.7	91.6	89.2	91.0	86.8	89.5	90.6
Thom (°C)															1045	1080	1040	1065	1040

* Mg# calculated using $Fe^{3+}/Fe^{2+} = 0.1$. Columns: 1 groundmass, 2–5 matrix glass, 6–14 naturally quenched glass inclusions, 15–19 experimentally homogenized and quenched glass inclusions. Thom: homogenization temperature. Groundmass composition is an average result of 12 randomly positioned broad-beam (50 × 30 μm) electron-microprobe analyses (Fig. 1). The composition of the host plagioclase was determined within 20 μm of the inclusions. Compositions are reported in wt.% oxides.

were checked using an optical microscope with high magnification (320×) for the absence of any visible cracks or other irregularities on their surfaces.

Plagioclase grains containing several primary glass inclusions >20 μm in diameter, completely enclosed within the host crystal, were studied experimentally using a low-thermal-inertia heating stage that allows visual control of experiments under the microscope (Sobolev & Danyushevsky 1994). Grains with inclusions consisting of glass only, or of glass and a fluid (shrinkage) bubble, were chosen for the experiments. Inclusions recrystallized at 600–700°C during heating, forming a non-transparent aggregate of microlites. At 850–900°C, the microlites began to melt, and at ~1000°C, all microlites had melted completely, yielding transparent inclusions consisting of melt and a bubble of fluid. Inclusions were heated over a period of ~1 minute above ~950°C until the moment of complete homogenization (disappearance of the bubble of fluid). Longer experimental times (lower heating rates at high temperatures) resulted in progressively higher temperatures of homogenization, a common feature of hydrous melts, probably caused by H_2O dissociation (Sobolev & Danyushevsky 1994). Visual control allows confident identification of "opened" inclusions, as such inclusions would leak during experiments (inclusions either decrepitate, or fluid bubble increases or shows no change in size with increasing temperature). Inclusions were quenched immediately after homogenization, and the sample was polished to expose the inclusion on the crystal surface for electron-microprobe analysis. The correctly established temperature of homogenization is believed to be the trapping (*i.e.*, crystallization) temperature for fluid-saturated melts (Sobolev & Danyushevsky 1994).

RESULTS

Mineralogy and petrology

High-Ca boninite suites recovered from the northern part of the Tonga Trench are characterized by a broad compositional spectrum (Falloon *et al.* 1987, Danyushevsky *et al.* 1995). Compositions of whole-rock and matrix glass in a suite recovered in dredge haul 3, station 21 (1500–2000 m water depth, Falloon & Crawford 1991) define coherent trends when plotted against MgO (Fig. 1). These trends are consistent with initial crystallization of olivine, followed by orthopyroxene and clinopyroxene (at 10–8 wt.% MgO), plagioclase (at 4–3 wt.% MgO) and magnetite (at 3–2 wt.% MgO). All these minerals occur as phenocrysts in the dredged samples. However, on the basis of variations in the number of distinct phenocryst phases (from 2 to 5), their proportions, and their total abundance (from <1 to ~40 vol.%), Falloon & Crawford (1991) distinguished six distinct rock types in this suite. Vesicularity of the samples varies widely with rock type, from near zero to ~30 vol.%, with no correlation with sample compositions. Large phenocrysts (up to 4 mm) of high-An plagioclase are present only in sample 3–24, although smaller and less abundant plagioclase phenocrysts and microphenocrysts of similar compositions were found in other samples (Falloon & Crawford 1991).

Sample 3–24 contains ~40 vol.% phenocrysts (olivine, orthopyroxene, clinopyroxene, plagioclase) set in fresh matrix glass with pyroxene microlites [zoned from orthopyroxene to subcalcic augite, Mg# 83–76; Mg# = 100*Mg/(Mg + Fe^{2+})] and ~10 vol.% vesicles (Falloon & Crawford 1991). Compositions of matrix glass and an estimate of the groundmass composition (liquid = matrix glass + pyroxene microlites) are shown in Table 1 and Figure 1; the latter is an average result of 12 randomly positioned broad-beam (50 × 30 μm) electron-microprobe analyses; the range of individual compositions (Fig. 1) reflects different proportions of matrix glass and microlites in the analyzed areas. As expected, the compositions of matrix glass form the low-Mg continuation of the compositional trend defined by individual compositions of the groundmass; this trend, characterized by constant Ca and increasing Si, Al, K, Na and Ti with decreasing Mg, is consistent with subtraction of low-Ca pyroxene from (or with its addition to) the groundmass composition.

Mineralogical features of sample 3–24 are summarized in Table 2 and Figure 2. Olivine phenocrysts are unzoned and have high forsterite contents (Fo_{88-89}). Compositions of orthopyroxene phenocrysts have a clear bimodal distribution. Magnesian crystals, with a Mg# of 86–89, are unzoned, whereas more evolved phenocrysts (core compositions with Mg# in the range 65–70) show normal zoning of up to 4 Mg# units. Clinopyroxene phenocrysts (core compositions with Mg# in the range 68–81) are normally zoned by 3–4 Mg# units. Most plagioclase phenocrysts are unzoned within analytical uncertainty, although occasional crystals show narrow oscillatory zones of up to 5 mol.% An.

Compositions of pyroxene inclusions in plagioclase phenocrysts and plagioclase inclusions in pyroxene phenocrysts (Table 2) indicate that plagioclase crystallized together with the most evolved pyroxene phenocrysts. We have also found magnetite inclusions in plagioclase phenocrysts, further supporting plagioclase crystallization from the evolved melts. Magnetite crystallization from these melts is also suggested by a sharp decrease in Ti and Fe concentration in most evolved melts (Fig. 1).

Low-density (with no identifiable liquid phase) H_2O-rich primary fluid inclusions in phenocrysts are a typical feature of boninites from the Tonga arc (Sobolev & Danyushevsky 1994). Such inclusions are interpreted to

TABLE 2. MINERALOGY OF SAMPLE 3-24*

	Ave. Mg# or An	Range of Mg# or An	No. of grains
Phenocrysts:			
Olivine (7%)	88.9	88.4-89.5	27
Orthopyroxene (17%)			
High-magnesium	88.3	85.6-89.2	11
Low-magnesium	68.7	65.7-70.6	16
Clinopyroxene (5%)	73.7	68.8-81.4	33
Plagioclase (10%)	89.3	82.2-94.2	108
Inclusions in Plagioclase:			
Orthopyroxene	66.9	65.9-70.0	14
Clinopyroxene	68.1	68.1-71.4	7
Plagioclase inclusions in:			
Orthopyroxene Mg# 66.2	89.1	-	1
Clinopyroxene Mg# 69.1	89.2	-	1

* Numbers in parentheses are modal percentages of phenocrysts (based on the counting of over 1000 points), from Falloon & Crawford (1991). Mg# = 100*Mg/(Mg + Fe^{2+}).

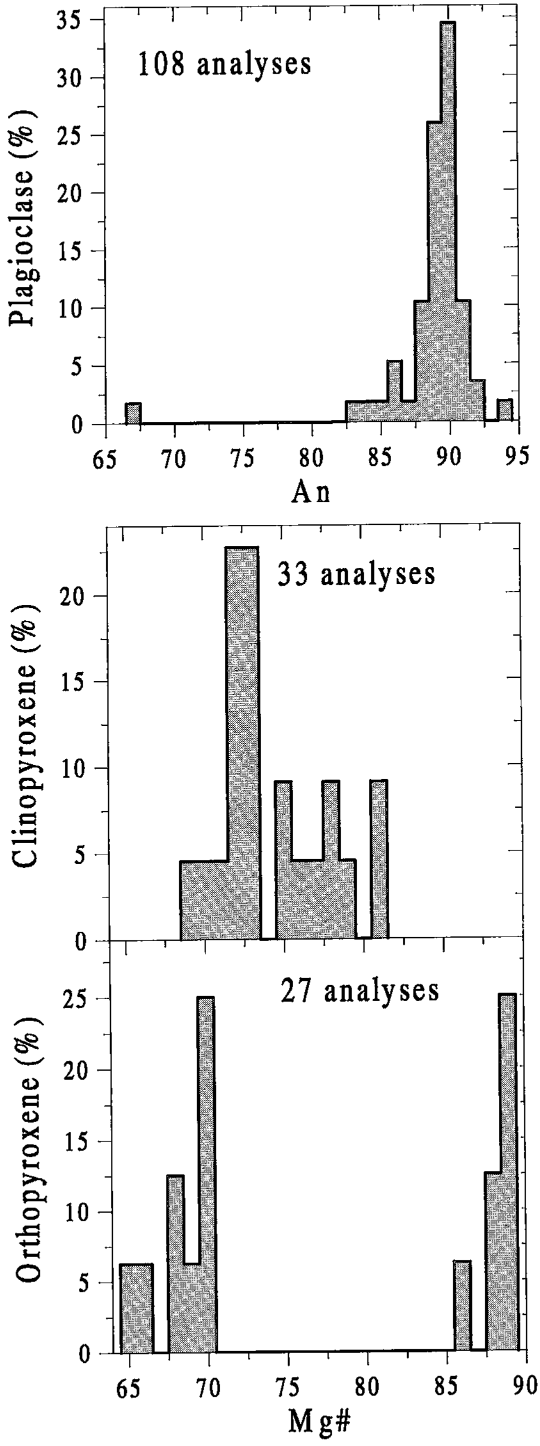

FIG. 2. Histograms of core compositions of plagioclase and pyroxene phenocrysts from sample 3–24.

reflect crystallization under low-pressure, H_2O-saturated conditions, as also suggested by the observation of high vesicularity in many samples. We have found primary fluid inclusions in all phenocryst phases of sample 3–24 [see previous section and Roedder (1984) for the criteria used to identify inclusions).

Glass inclusions in plagioclase phenocrysts

Compositions of naturally quenched glass inclusions in plagioclase phenocrysts (Table 1) are dacitic and form the low-Mg continuation of the compositional trend defined by this suite; the most Mg-rich compositions

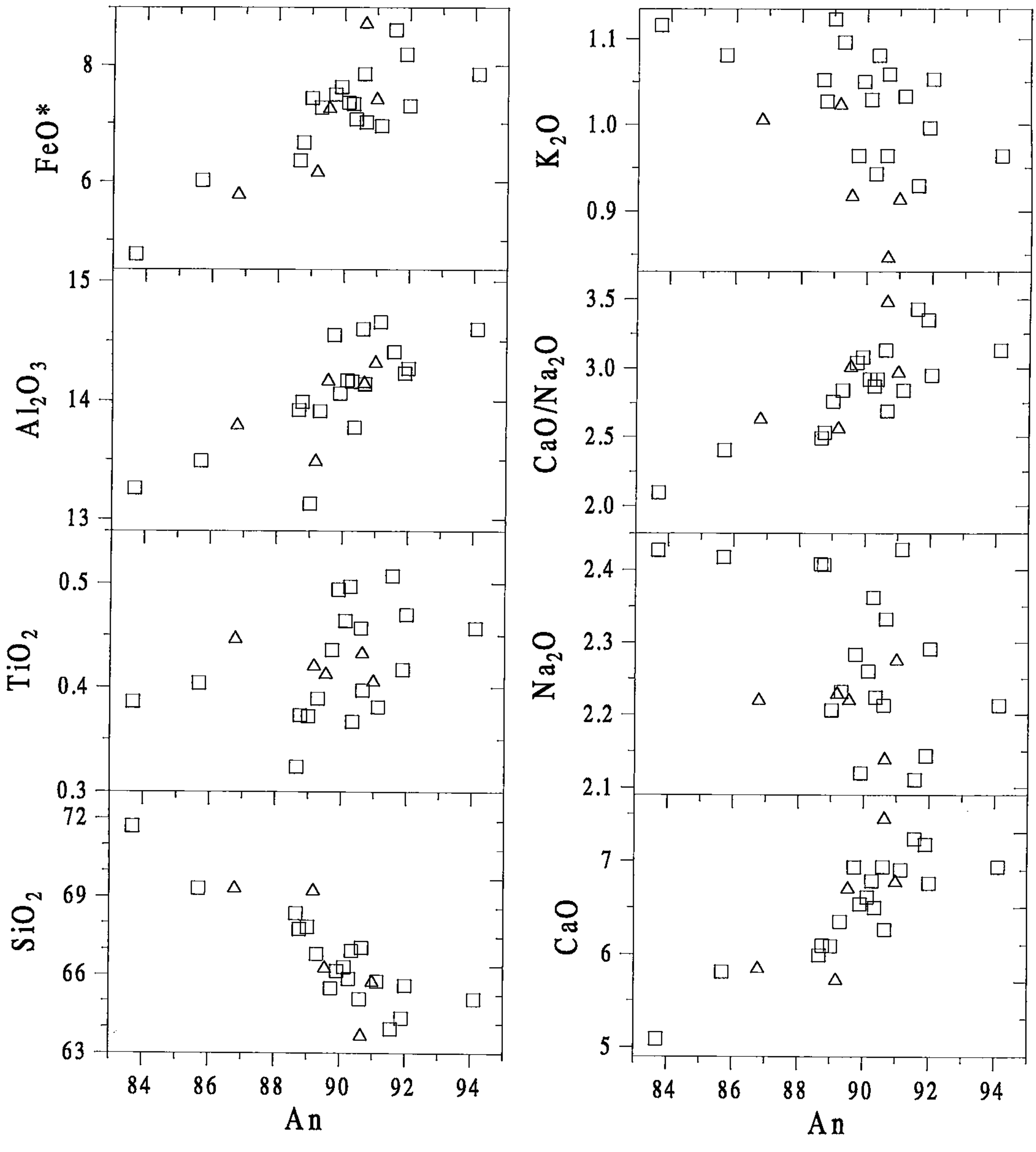

FIG. 3. Compositions of homogenized and quenched, and naturally quenched, glass inclusions in plagioclase phenocrysts from sample 3–24. Symbols as on Fig. 1.

found in inclusions are close to the whole-rock compositions of the most evolved members of the suite (Fig. 1). Fe, Ti, K, and Na are similar in inclusions and matrix glass, but the inclusions show a sharper increase in Si and a decrease in Ca and Al contents with decreasing Mg. Crystallization of plagioclase on the walls of these inclusions could only increase Mg contents of the residual melt within inclusions, and thus such inclusions provide an upper limit in Mg of the melts that crystallized plagioclase phenocrysts. An important implication of this observation is that high-An plagioclase crystallized from melts with the lowest Ca/Na values for this suite. The H_2O contents of these inclusions (1.4–1.6 wt.%, Table 2), established by FTIR, do not show significant variations and match those in the evolved melts of the Tongan suite of high-Ca boninite (Sobolev & Danyushevsky 1994, Danyushevsky *et al.* 1995).

Compositions of plagioclase-hosted melt inclusions that were homogenized during heating experiments are listed in Table 1. Homogenization of the inclusions was observed at temperatures between 1040–1080°C. This temperature range is within the accuracy of the experimental technique (±20°C), and no correlation has been established between homogenization temperature and plagioclase composition. Compositions of homogenized inclusions are indistinguishable from the compositions of unheated inclusions, implying that no significant crystallization of plagioclase occurred on the walls of naturally quenched glass inclusions. A good correlation exists between the compositions of melt inclusions and of host plagioclase (Fig. 3). This applies for both unheated and homogenized melt inclusions, and is consistent with the liquid line of descent during crystallization of pyroxene + plagioclase + magnetite (Fig. 3).

DISCUSSION

Pre-eruption history of sample 3–24

The bulk composition of sample 3–24 (Table 3) is anomalous when compared with compositional trends defined by the suite of samples recovered from station 23 (Fig. 1). Most notably, this sample has high Si and low Ca, Fe, and Al compared with other samples of similar Mg content (Fig. 1). This does not necessarily imply that this sample is unrelated to the rest of the suite. Instead, its anomalous composition can be explained by the phenocryst-rich nature of this sample, which implies that the bulk composition is not representative of a liquid composition, and is better explained by the accumulation of crystals prior to eruption. Indeed, a mass-balance calculation (Table 3) demonstrates that the whole-rock composition of sample 3–24 can be produced by a combination of phenocrysts and the groundmass, in proportions that closely match those obtained during point counting (Table 2).

The composition of the erupted melt (now groundmass, *i.e.*, glass + microphenocrysts) that transported phenocrysts during eruption also is anomalous when compared with the rest of the samples recovered from station 23. It has a higher Mg content than melts (represented by melt inclusions) that crystallized plagioclase and low-Mg (Mg# < 72) pyroxene phenocrysts; and has high Si and low Ca, Fe, and Al compared with the samples of similar Mg content from this suite. Pyroxene microlites from sample 3–24, which crystallized from the transporting melt, are more magnesian than pyroxene phenocrysts that crystallized together with high-An plagioclase (which is consistent with higher Mg content of the transporting melt

TABLE 3. MAJOR ELEMENT MODELING OF PHENOCRYST ACCUMULATION IN SAMPLE 3-24*

	Average plagioclase	Average high-Mg# orthopyroxene	Average low-Mg# orthopyroxene	Average clinopyroxene	Average olivine	Groundmass (Table 1)	Sample 3-24 calculated	Sample 3-24 observed
SiO_2	45.68	57.22	53.02	52.50	40.74	65.50	59.35	59.35
TiO_2	-	.02	0.11	0.17	-	0.39	0.25	0.25
Al_2O_3	33.93	.52	1.06	2.05	-	13.14	10.99	10.99
FeO*	1.06	7.96	19.56	10.15	10.77	7.63	8.85	8.85
MgO	0.08	33.86	24.11	15.76	48.34	3.16	10.83	10.83
CaO	18.04	1.38	1.84	19.13	0.14	7.01	7.80	7.80
Na_2O	1.20	.02	0.02	0.13	-	2.23	1.39	1.37
K_2O	0.00	-	-	-	-	0.93	0.53	0.56
Mg# or An	89.2	88.3	68.7	73.5	88.9			
Amount (wt.%)	9.4	9.5	12.5	9.3	2.9	56.4	100	-
Amount (vol.%)	9.1	7.5	9.9	7.4	2.3	63.9	100	-

* Calculations were performed using a least-squares linear-approximation model (Wright & Doherty 1970). The sum of the squares of the residuals is equal to 0.002. Compositions of average plagioclase, clinopyroxene, orthopyroxene and olivine pertain to real phenocrysts, which match the compositions reported in Table 2. The whole-rock composition of sample 3-24 is taken from Falloon & Crawford (1991). Volume % values were calculated using a density of 3.30 $g \cdot cm^{-3}$ for olivine and the pyroxenes, 2.70 $g \cdot cm^{-3}$ for plagioclase, and 2.30 $g \cdot cm^{-3}$ for the groundmass (Deer *et al.* 1966, Newman *et al.* 1986). Mg# = 100*Mg/(Mg + Fe^{2+}). Compositions are expressed in wt.% oxides.

compared to those melts in equilibrium with plagioclase). The pyroxene microphenocrysts are also significantly less magnesian than olivine and high-Mg# orthopyroxene phenocrysts. All of these observations imply disequilibrium between phenocrysts and the transporting melt. The composition of the transporting melt is best explained as the product of mixing, in a shallow, open-system magma chamber, of an evolved melt, represented by melt inclusions in plagioclase, and a less evolved, more magnesian melt. The Mg content of the melt in equilibrium with olivine Fo_{89} along the liquid line of descent for the suite from station 23 is ~11.7 wt.% MgO (assuming olivine– melt K_D = 0.3, FeO* = 9.5 wt.%, Fe^{3+}/Fe^{2+} = 0.1) As can be estimated from Figure 1, the groundmass composition can be produced by mixing of ~85% of an evolved melt having ~1.7 wt.% MgO with 15% of a more primitive melt containing ~11.7 wt.% MgO. Following this scenario, magnesian olivine and orthopyroxene phenocrysts crystallized from the high-Mg melt prior to mixing, whereas plagioclase and low-magnesium (Mg# < 72) pyroxene phenocrysts crystallized from the evolved melts. Phenocrysts of more magnesian clinopyroxene from sample 3–24 either crystallized from the transporting melt after mixing and prior to eruption, or were trapped by the transporting melt from a crystal mush in the magma chamber.

Plagioclase–melt equilibrium

The results of our study indicate that phenocrysts of calcic plagioclase crystallized at the latest stages of melt evolution from H_2O-saturated dacitic melts (SiO_2 64–67 wt.%, MgO ~2 wt.%) at ~1050°C and low pressure [~0.25 kilobar, on the basis of the H_2O solubility model of Moore *et al.* (1995)]. These melts contained ~1.5 wt.% H_2O and had low CaO/Na_2O values (~3).

It seems clear that the presence of high-An plagioclase in subduction-related magmas does not necessarily imply either high melt H_2O contents (>6 wt.%), or high CaO/Na_2O values (>8) of the melt, as was previously suggested (Falloon & Green 1986, Falloon & Crawford 1991, Panjasawatwong *et al.* 1995).

Our results also raise significant questions concerning current models of plagioclase–melt equilibrium. The compositions of coexisting plagioclase and dacitic melt from the Tongan suite, and comparable data from H_2O-saturated experiments (Housh & Luhr 1991, Sisson & Grove 1993) are shown in Figure 4. The H_2O-saturated experiments were performed at pressures of 2–4 kilobars on broadly dacitic to basaltic melt compositions containing 6–10 wt.% H_2O. These experiments form a coherent trend in terms of An *versus* Ca/Na values of the melt, regardless of pressure and H_2O contents. Plagioclase phenocrysts from the Tongan suite correspond to the experimental trend of the H_2O-saturated runs, overlapping with the 2 kbar H_2O-saturated experiments of Sisson & Grove (1993), although H_2O contents of Tongan melts were significantly lower during crystallization, reflecting the lower pressure of crystallization. A comparison of glass-inclusion compositions in Tongan plagioclase phenocrysts with the glass compositions in the experiments of Sisson & Grove (1993) (Fig. 5) shows that for similar plagioclase compositions in the experiments, calcic plagioclase phenocrysts from sample 3–24 crystallized at slightly higher temperature (~50°C), from melts with significantly higher Si and lower H_2O, Al, Mg, Ca, and Na contents, but identical Ca/Na values. This observation is somewhat surprising, as current understanding of hydrous melt – plagioclase equilibrium (*e.g.*, Housh & Luhr 1991) indicates that lower H_2O contents of the melt at a given Ca/Na value should produce lower An in the equilibrium plagioclase. Moreover, on the basis of models of anhydrous melt–plagioclase equilibrium (*e.g.*, Grove *et al.* 1992, Panjasawatwong *et al.* 1995), the observed lower Al/Si values at a given Ca/Na value in melt inclusions in plagioclase from sample 3–24, compared to the experiments of Sisson & Grove (1993), should also lead to a significant decrease of the An content of the equilibrium plagioclase. At the same time, a small increase in temperature of crystallization and decrease in pressure of crystallization produce only a slight increase in the An content of equilibrium plagioclase (Grove *et al.* 1992, Panjasawatwong *et al.* 1995).

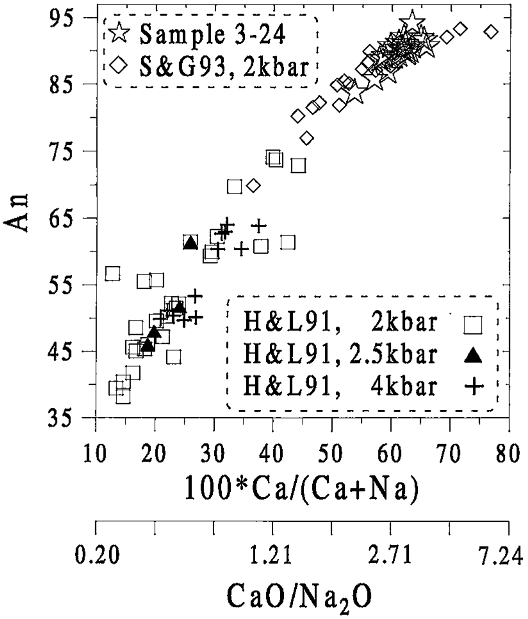

FIG. 4. Anorthite contents of liquidus plagioclase *versus* melt CaO/Na_2O value for H_2O-saturated experiments and plagioclase phenocrysts from sample 3–24. S&G93: Sisson & Grove (1993); H&L91: Housh & Luhr (1991). See text for discussion.

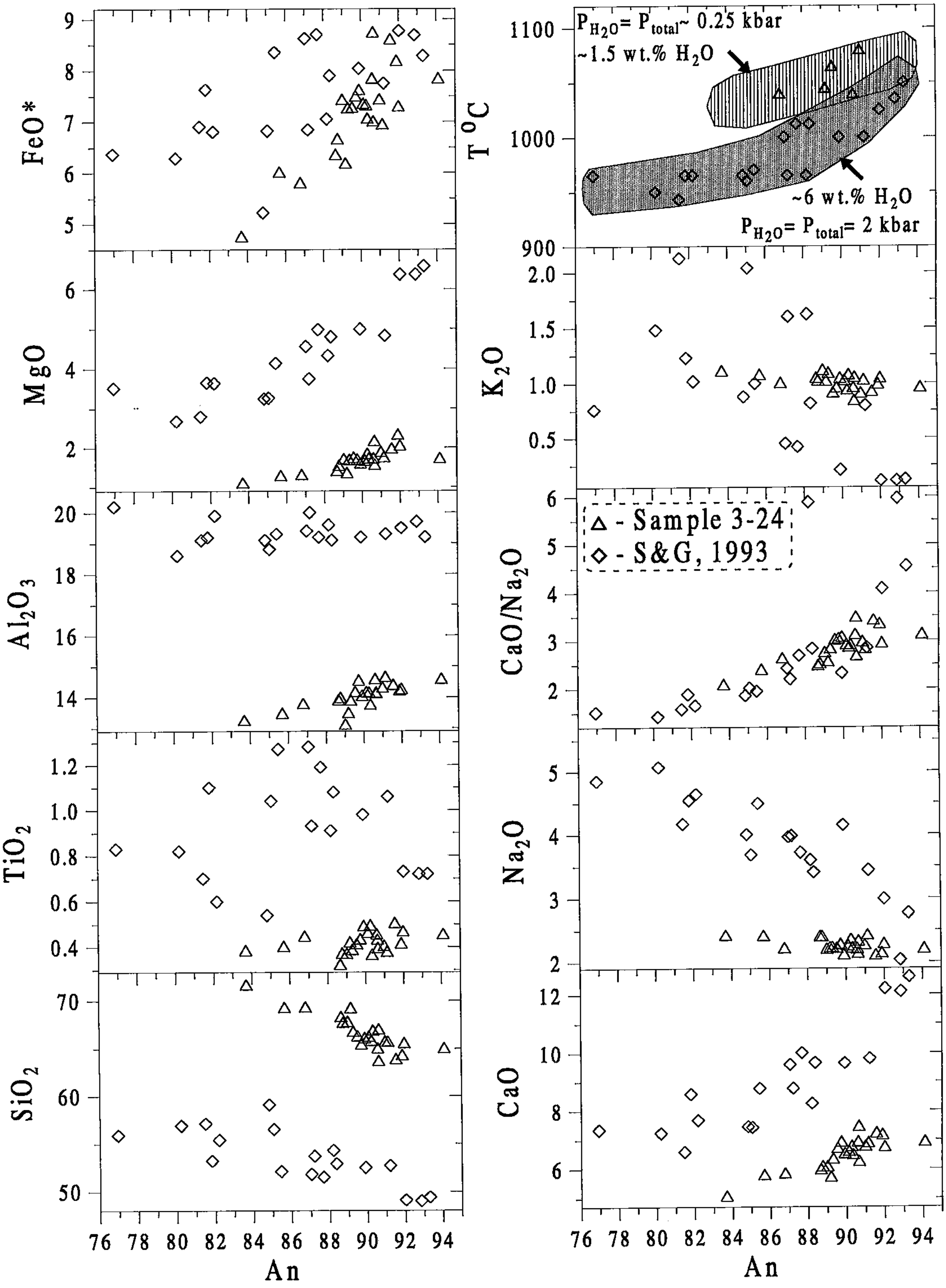

FIG. 5. Comparison of melt compositions in equilibrium with high-An plagioclase, and conditions of crystallization of high-An plagioclase in experiments of Sisson & Grove (1993) and in Tongan boninite. See text for discussion.

Housh & Luhr (1991) presented a thermodynamic model of plagioclase–melt equilibria in which albite and anorthite components are described through the use of separate equilibrium constants (K_{An} and K_{Ab}, Fig. 6). These calculated equilibrium constants account for the effects of pressure and H_2O content of the melt on the component activities in the melt and plagioclase, and are linearly dependent on inverse temperature. The Housh & Luhr (1991) model is based on a combination of the regular solution model for activities of components in the hydrous melt, as formulated by Ghiorso *et al.* (1983), and the plagioclase model of Fuhrman & Lindsley (1988). The "hydrous" part of the Ghiorso *et al.* (1983) model is based largely on the intermediate to felsic compositions investigated experimentally under H_2O-saturated conditions, generally at pressures above 1 kbar; Housh & Luhr (1991) calibrated their model on the basis of experiments performed under H_2O-saturated conditions at 2 to 4 kilobar on rhyolitic to dacitic melt compositions [$K_{Ab} = -4.365 + 18571.1 / T(K)$, $K_{An} = -4.627 + 25689.8 / T(K)$, Fig. 6]. Housh & Luhr (1991) claimed that their formulation of plagioclase–melt equilibrium can be applied to a broader range of compositions, including basalts and andesites, at anhydrous and H_2O-undersaturated conditions (see their Fig. 7). However, as can be seen in Figure 6A, there is no unique correlation between temperature and K_{An} [in the form defined by the experimental results of Housh & Luhr (1991), their Figure 6]. All anhydrous experiments in the pressure range from 1 atmosphere to 20 kilobars over a broad compositional spectrum (see caption of Figure 6 for details) form a tight trend parallel to that formed by the H_2O-saturated experiments, but corresponds to lower K_{An} values. The H_2O-undersaturated experiments display K_{An} values intermediate between the anhydrous and H_2O-saturated experiments for a given temperature (note that because the value of K_{An} is sensitive to H_2O content of the melt, the position of the undersaturated experiments on Figure 6 is not so well constrained owing to uncertainties in H_2O contents of H_2O-undersaturated experiments). The albite model does not display a systematic shift in K_{Ab} between anhydrous and H_2O-saturatated experiments, but instead shows significant scatter at higher temperatures compared with the relatively good linear correlation defined by the experiments run at the lowest temperatures (Fig. 6B).

The reasons for the deviations of anhydrous and H_2O-undersaturated experiments from the K_{An} trend as defined by the H_2O-saturated experiments, and for the failure of the albite model to produce a good linear relation between ln (K_{Ab}) and 1/T for anhydrous and H_2O-undersaturated experiments, can either lie in a dependence of the activities of albite and anorthite in plagioclase on H_2O pressure, or in the formulation of melt-component activities for hydrous melts in the model of Ghiorso *et al.* (1983). We do not expect that

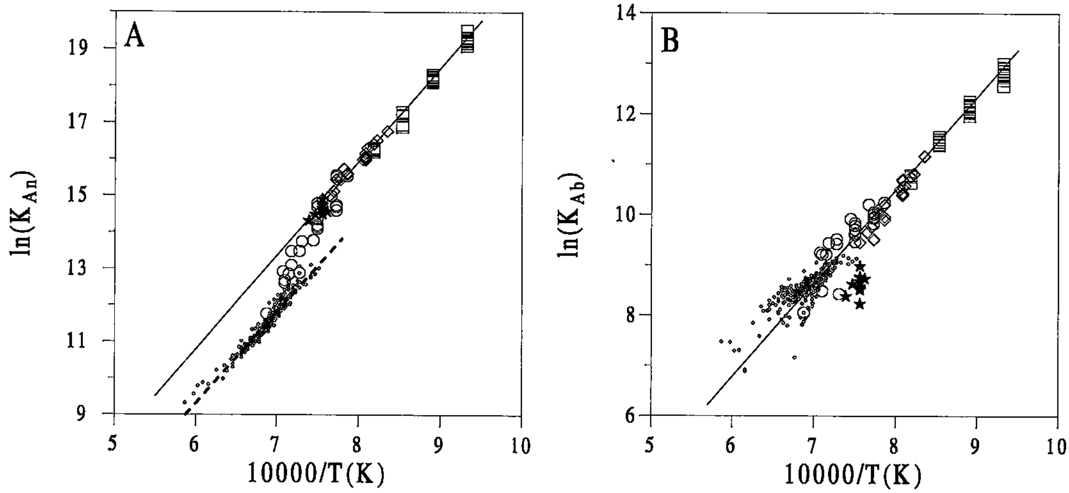

FIG. 6. Application of the anorthite-melt (A) and albite-melt (B) models of Housh & Luhr (1991) to anhydrous and H_2O-bearing experiments and plagioclase phenocrysts from sample 3–24. A. Plot of ln (K_{An}) *versus* 10000/T (K). B. Plot of ln (K_{Ab}) *versus* 10000/T (K). Stars: sample 3-24; solid lines represent the formulation of the model (Housh & Luhr 1991), which is based on H_2O-saturated experiments; small circles: anhydrous experiments from Bender *et al.* (1978), Walker *et al.* (1979), Stolper (1980), Grove *et al.* (1982), Grove & Bryan (1983), Baker & Eggler (1987), Duncan & Green (1987), Sack *et al.* (1987), Tormey *et al.* (1987), Grove & Juster (1989), Juster *et al.* (1989), Thy (1991), Thy *et al.* (1991), Fram & Longhi (1992), Grove *et al.* (1992); large circles: H_2O-undersaturated experiments from Panjasawatwong *et al.* (1995) and Baker & Eggler (1987); H_2O-saturated experiments: diamonds: Sisson & Grove (1993); squares: Housh & Luhr (1991). The relationship between K_{An} and T for the anhydrous conditions is $K_{An} = -5.724 + 25044.3 / T(K)$ ($R^2 = 0.942$). See text for discussion.

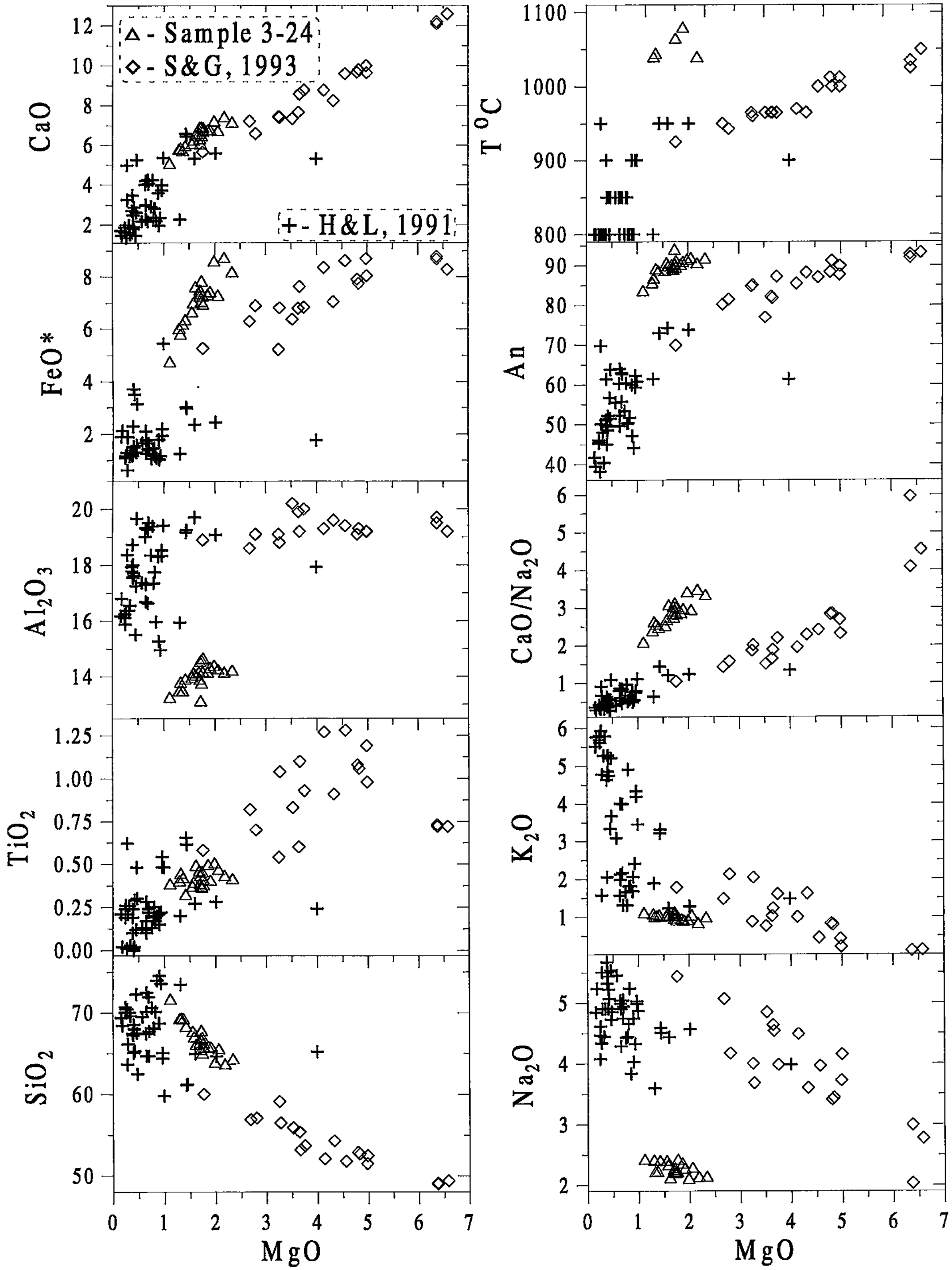

FIG. 7. Comparison of melt compositions from H_2O-saturated experiments of Housh & Luhr (1991) and Sisson & Grove (1993), which are successfully described by the model of plagioclase–melt equilibrium of Housh & Luhr (1991), with melt compositions from Tongan boninite suite in equilibrium with high-An plagioclase. See text for discussion.

activities of components in the plagioclase crystals will be significantly affected by the presence of H_2O in the melt from which they grow, and therefore suggest that the major source of uncertainty is in the regular solution model for hydrous melts, especially those with low H_2O contents. This is likely not due to any fundamental fault in the Ghiorso *et al.* (1983) melt model, but simply a reflection of a limited number of experiments on hydrous compositions (all of which are H_2O-saturated) in the database on which the Ghiorso *et al.* (1983) model relies. Also, the observed systematic shift between anhydrous and H_2O-saturated anorthite–melt equilibria (Fig. 6A) likely reflects the non-consistency of models proposed by Ghiorso *et al.* (1983) for anhydrous and hydrous melts.

Despite the problems discussed above, the model of Housh & Luhr (1991) successfully reproduces the 2 kbar H_2O-saturated experiments of Sisson & Grove (1993) (Fig. 6), which have similar H_2O contents, but significantly different liquid compositions and temperatures from those used to derive the model (Fig. 7).

However, when applied to H_2O-saturated evolved Tongan boninites, the model predictions are not consistent. The anorthite-based model agrees quite well with our observations on the Tongan boninite, but the albite–melt model predicts ~6 wt.% H_2O in the evolved Tongan boninitic melt, if it is to crystallize high-An plagioclase (Fig. 6). As follows from our analysis, anorthite activity in equilibrium melt and plagioclase is correctly described by the combination of Ghiorso *et al.* (1983) and Fuhrman & Lindsley (1988) for all H_2O-saturated compositions shown on Figure 7, whereas these models cannot describe albite activity during the crystallization of Tongan boninites, which should be lower in the melt compared to that predicted by Ghiorso *et al.* (1983). It is generally known that melt properties such as viscosity and solidus temperature (freezing-point depression) are strongly nonlinear functions of H_2O content of the melt (*e.g.*, Burnham 1979, Schulze *et al.* 1996). Therefore, it may not be too surprising that a model calibrated at relatively high H_2O contents does not do very well in predicting plagioclase–melt equilibria at low pressures and low H_2O contents of the melt.

To emphasize compositional differences between evolved Tongan boninitic melts in equilibrium with high-An plagioclase and experimental liquids of Housh & Luhr (1991) and Sisson & Grove (1993), we compared them on Figure 7. Most significantly, the Tongan boninitic melts differ from experimental liquids by lower Al, Na, and H_2O contents and higher temperature at a given Mg. Additional experimental data at low H_2O contents are required to address this problem quantitatively.

CONCLUSIONS

New mineralogical and melt-inclusion data on a unique sample from a suite of high-Ca boninites suggests a complex petrological history that has involved mixing of evolved magma with a small amount (~15 wt%) of much more mafic material consisting of ~50% primitive (>11% MgO) melt and magnesian olivine and orthopyroxene. Melt inclusions in $An_{>90}$ plagioclase present in this mixed magma show a good correlation with the An content of the enclosing plagioclase, supporting the view that these inclusions provide good samples of the melt from which such unusually calcic plagioclase crystallized. We conclude that plagioclase crystallized at the latest stages of melt evolution from H_2O-saturated dacitic melts (SiO_2 64–67 wt.%, MgO ~2 wt.%) at temperatures ~1050°C and low pressure (<1 kbar). These melts contained ~1.5 wt.% H_2O and had low CaO/Na_2O (~3).

An important conclusion of this study is that the presence of phenocrysts of high-Ca plagioclase in arc lavas does not necessarily imply high H_2O contents in the melt or involvement of refractory, high-(Ca/Na) melts in magma genesis.

When the Housh & Luhr (1991) model of plagioclase–melt equilibria is applied to these samples, the An-based model yields relatively good agreement with our measurements on H_2O contents of the inclusions, whereas the Ab-based model predicts H_2O contents of ~6 wt% in the melt. This discrepancy suggests that currently available models of the effect of H_2O on the activities of plagioclase components in evolved melts may be in error when extrapolated to low activities of H_2O and low $P(H_2O)$; this likely reflects the strongly nonlinear correlations between H_2O content of the melt and component activities, as suggested by available data on phase equilibria (*e.g.*, freezing-point depression) and physical properties (*e.g.*, viscosity, electrical conductivity). There clearly is a need for more experimental data at low pressures and low H_2O contents of relevant melts for use in developing more robust models, needed to make predictions of H_2O activities in the magma from measurements of mineral–melt equilibria.

ACKNOWLEDGEMENTS

This research was supported by an Australian Research Council Large grant to LVD and TJF, an ARC PDRF to LVD, a Royal Society Endeavour Fellowship to TJF, and European Science Foundation, Environment Program (PRE–ERUPT) and Nuffield Foundation grants to MRC. We thank Dima and Maya Kamenetsky for assistance with melt-inclusion preparation for FTIR analyses, and Tony Crawford for useful critical comments. Critical reviews of J. Luhr, R. Nielsen, and R. Martin have significantly improved the original version of this paper.

REFERENCES

BAKER, D.R. & EGGLER, D.H. (1987): Compositions of anhydrous and hydrous melts coexisting with plagioclase, augite, and olivine or low-Ca pyroxene from 1 atm to 8 kbar: application to the Aleutian volcanic center of Atka. *Am. Mineral.* **72**, 12-28.

Bender, J.F., Hodges, F.N. & Bence, A.E. (1978): Petrogenesis of basalts from the project FAMOUS area: experimental study from 0 to 15 kbars. *Earth Planet. Sci. Lett.* **41**, 277-302.

Burnham, C.W. (1979): Magmas and hydrothermal fluids. *In* Geochemistry of Hydrothermal Ore Deposits 2 (H.L. Barnes, ed.). John Wiley and Sons, New York, N.Y. (71-136).

Danyushevsky, L.V., Falloon, T.J., Sobolev, A.V., Crawford, A.J., Carroll, M. & Price, R.C. (1993): The H_2O content of basalt glasses from southwest Pacific backarc basins. *Earth Planet. Sci. Lett.* **117**, 347-362.

________, Sobolev, A.V. & Falloon, T.J. (1995): North Tongan high-Ca boninite petrogenesis: the role of Samoan plumes and subduction zone – transform fault transition. *J. Geodynamics* **20**, 219-241.

Deer, W.A, Howie, R.A. & Zussman, J. (1966): *An Introduction to the Rock-Forming Minerals.* John Wiley and Sons, New York, N.Y.

Duncan, R.A. & Green, D.H. (1987): The genesis of refractory melts in the formation of oceanic crust. *Contrib. Mineral. Petrol.* **96**, 326-342.

Falloon, T.J. & Crawford, A.J. (1991): The petrogenesis of high-calcium boninite lavas dredged from the north Tonga ridge. *Earth Planet. Sci. Lett.* **102**, 375-394.

________ & Green, D.H. (1986): Glass inclusions in magnesian olivine phenocrysts from Tonga: evidence for highly refractory parental magmas in the Tongan arc. *Earth Planet. Sci. Lett.* **81**, 95-103.

________, ________ & Crawford, A.J. (1987): Dredged igneous rocks from the northern termination of the Tofua magmatic arc, Tonga and adjacent Lau Basin. *Aust. J. Earth Sci.* **34**, 487-506.

Fram, M.S. & Longhi, J. (1992): Phase equilibria of dikes associated with Proterozoic anorthosite complexes. *Am. Mineral.* **77**, 605-616.

Fuhrman, M.L. & Lindsley, D.H. (1988): Ternary-feldspar modelling and thermometry. *Am. Mineral.* **73**, 201-215.

Ghiorso, M.S., Carmichael, I.S.E., Rivers, M.L. & Sack, R.O. (1983): The Gibbs free energy of mixing of natural silicate liquids; an expanded regular solution approximation for the calculation of magmatic intensive variables. *Contrib. Mineral. Petrol.* **84**, 107-145.

Grove, T.L. & Bryan, W.B. (1983): Fractionation of pyroxene-phyric MORB at low pressure: an experimental study. *Contrib. Mineral. Petrol.* **84**, 293-309.

________, Gerlach, D.C. & Sando, T.W. (1982): Origin of calc-alkaline series lavas at Medicine Lake volcano by fractionation, assimilation and mixing. *Contrib. Mineral. Petrol.* **80**, 160-182.

________ & Juster, T.C. (1989): Experimental investigation of low-Ca pyroxene stability and olivine–pyroxene–liquid equilibria at 1-atm in natural basaltic liquids. *Contrib. Mineral. Petrol.* **103**, 287-305.

________, Kinzler, R.J. & Bryan, W.B. (1992): Fractionation of mid-ocean ridge basalt (MORB). *In* Mantle Flow and Melt Generation at Mid-Ocean Ridges. *Am. Geophys. Union, Geophys. Monogr.* **71**, 281-310.

Housh, T.B. & Luhr, J.F. (1991): Plagioclase–melt equilibria in hydrous systems. *Am. Mineral.* **76**, 477-492.

Jarosewich, E., Nelen, J.A. & Norberg, J.A. (1980): Reference samples for electron microprobe analyses. *Geostandards Newsletter* **4**. 257-258.

Juster, T.C., Grove, T.L. & Perfit, M.R. (1989): Experimental constraints on the generation of FeTi basalts, andesites and rhyodacites at the Galapagos Spreading Center, 85°W and 95°W. *J. Geophys. Res.* **94**, 9251-9274.

Kimata, M., Hishida, N., Shimizu, M., Saito, S., Matsui, T. & Arakawa, Y. (1995): Anorthite megacrysts from island arc basalts. *Mineral. Mag.* **59**, 1-14.

Moore, G., Vennemenn, T. & Carmichael, I.S.E. (1995): Solubility of water in magmas to 2 kbar. *Geology* **23**, 1099-1102.

Newman, S., Stolper, E.M. & Epstein, S. (1986): Measurement of water in rhyolitic glasses: calibration of an infrared spectroscopic technique. *Am. Mineral.* **71**, 1527-1541.

Nielsen, C.H. & Sigurdsson, H. (1981): Quantitative methods for electron microprobe analysis of sodium in natural and synthetic glasses. *Am. Mineral.* **66**, 547-552.

Panjasawatwong, Yuenyong, Danyushevsky, L.V., Crawford, A.J. & Harris, K.L. (1995): An experimental study of the effects of melt composition on plagioclase-melt equilibria at 5 and 10 kbar: implications for the origin of magmatic high-An plagioclase. *Contrib. Mineral. Petrol.* **118**, 420-432.

Roedder, E. (1984): Fluid inclusions. *Rev. Mineral.* **14**.

Sack, R.O., Walker, D. & Carmichael, I.S.E. (1987): Experimental petrology of alkalic lavas: constraints on cotectics of multiple saturation in natural basaltic liquids. *Contrib. Mineral. Petrol.* **96**, 1-23.

Schulze, F., Behrens, H., Holtz, F., Roux, J. & Johannes, W. (1996): The influence of H_2O on the viscosity of a haplogranitic melt. *Am. Mineral.* **81**, 1155-1165.

Sinton, C.W., Christie, D.M., Coombs, V.L., Nielsen, R.L. & Fisk, M.R. (1993): Near primary melt inclusions in anorthite phenocrysts from the Galapagos Platform. *Earth Planet. Sci. Lett.* **119**, 527-537.

Sisson, T.W. & Grove, T.L. (1993): Experimental investigations of the role of H_2O in calc-alkaline differentiation and subduction zone magmatism. *Contrib. Mineral. Petrol.* **113**, 143-166.

SOBOLEV, A.V. & DANYUSHEVSKY, L.V. (1994): Petrology and geochemistry of boninites from the north termination of the Tonga Trench: constraints on the generation conditions of primary high-Ca boninite magmas. *J. Petrol.* **35**, 1183-1211.

STOLPER, E. (1980): A phase diagram for mid-ocean ridge basalts: preliminary results and implications for petrogenesis. *Contrib. Mineral. Petrol.* **74**, 13-27.

THY, P. (1991): High and low pressure phase equilibria of a mildly alkalic lava from the 1965 Surtsey eruption: experimental results. *Lithos* **26**, 223-243.

________, LOFGREN, G.E. & IMSLAND, P. (1991): Melting relations and the evolution of the Jan Mayen magma system. *J. Petrol.* **32**, 303-332.

TORMEY, D.R., GROVE, T.L. & BRYAN, W.B. (1987): Experimental petrology of normal MORB near the Kane Fracture Zone – 22°–25° N, mid-Atlantic ridge. *Contrib. Mineral. Petrol.* **96**, 121-139.

WALKER, D.A., SHIBATA, T. & DELONG, S.E. (1979): Abyssal tholeiites from the Oceanographer Fracture Zone. II. Phase equilibria and mixing. *Contrib. Mineral. Petrol.* **70**, 111-125.

WRIGHT T.L. & DOHERTY, P.C. (1970): A linear programming and least squares computer method for solving petrologic mixing problems. *Geol. Soc. Am. Bull.* **81**, 1995-2008.

Received November 27, 1995, revised manuscript accepted February 7, 1997.